Composition control and thickness dependence of {100}-oriented epitaxial BiCoO3-BiFeO3 films grown by metalorganic chemical vapor deposition

doi: 10.1063/1.3073824

Composition control and thickness dependence of {100}-oriented epitaxial $BiCoO_3$–$BiFeO_3$ films grown by metalorganic chemical vapor deposition

Shintaro Yasui,[1] Mitsumasa Nakajima,[1] Hiroshi Naganuma,[2] Soichiro Okamura,[2] Ken Nishida,[3] Takashi Yamamoto,[3] Takashi Iijima,[4] Masaki Azuma,[5] Hitoshi Morioka,[1,6] Keisuke Saito,[6] Mutsuo Ishikawa,[1] Tomoaki Yamada,[1] and Hiroshi Funakubo[1,a)]

[1]*Department of Innovative and Engineered Materials, Tokyo Institute of Technology, J2-1508, 4259 Nagatsuta-cho, Midori-ku, Yokohama 226-8502, Japan*

[2]*Department of Applied Physics, Tokyo University of Science, 1-3 Kagurazaka, Shinjyuku-ku, Tokyo 162-8601, Japan*

[3]*Department of Communications Engineering, National Defense Academy, 1-10-20 Hashirimizu, Yokosuka, Kanagawa 239-8686, Japan*

[4]*Resarch Center for Hydrogen Industrial Use and Storage, National Institute of Advance Industrial Science and Technology, 1-1-1 Umezono, Tsukuba, Ibaraki 305-8568, Japan*

[5]*Institute for Chemical Research, Kyoto University, Gokasyo, Uji, Kyoto 611-0011, Japan*

[6]*Application Laboratory, Bruker AXS, 3-9-A Moriya-cho, Kanagawa-ku, Yokohama, Kanagawa 221-0022, Japan*

(Received 16 July 2008; accepted 29 December 2008; published online 16 March 2009)

xBiCoO$_3$–$(1-x)$BiFeO$_3$ films were deposited by metalorganic chemical vapor deposition. Although the film composition changed with deposition temperature, the composition could be adjusted by varying the input source gas composition at 700 °C. Moreover, adjusting the deposition time could change 0.16BiCoO$_3$–0.84BiFeO$_3$ film thickness. The crystal symmetry changed from rhombohedral to tetragonal as the film thickness decreased for 0.16BiCoO$_3$–0.84BiFeO$_3$ films grown on both (100)SrTiO$_3$ and $(100)_c$SrRuO$_3$‖(100)SrTiO$_3$ substrates, implying that the x value of the crystal symmetry boundaries between the tetragonal and rhombohedral structures changes with film thickness. © *2009 American Institute of Physics*. [DOI: 10.1063/1.3073824]

I. INTRODUCTION

Recently, environmental-friendly lead-free piezoelectric materials have been widely investigated.[1–4] In particular, alkali metal-based piezoelectric materials, e.g., (K,Na)NbO$_3$, (K,Na,Li)(Nb,Ta,Sb)O$_3$, etc., show good piezoelectricity.[2,4] However, these materials contain alkali metals, which are not suitable for film forms of microelectromechanical system (MEMS) applications integrated on Si substrates. Therefore, a novel candidate for lead-free piezoelectric materials without alkali metals is required, especially for MEMS applications.

We have examined bismuth-based perovskite materials as potential candidates due to the chemical similarity between Pb and Bi and have proposed a BiCoO$_3$–BiFeO$_3$ solid solution system.[5–7] This system has a phase boundary between tetragonal and rhombohedral symmetries through an intermediate monoclinic symmetry, similar to a PbTiO$_3$-based system with a large piezoelectricity, such as PbTiO$_3$–PbZrO$_3$, PbTiO$_3$–Pb(Zn$_{1/3}$Nb$_{2/3}$)O$_3$, and PbTiO$_3$–Pb(Mg$_{1/3}$Nb$_{2/3}$)O$_3$.[8,9]

In our previous study, we reported the crystal symmetry change with film composition x in xBiCoO$_3$–$(1-x)$BiFeO$_3$ for 200 and 400 nm thick films and found that the crystal symmetry differed between these film thicknesses around $x=0.16$ composition.[5,6] Hence, a crystal symmetry change occurs at a film thickness near this composition.

Herein we mainly focused on the film thickness dependency of the crystal structure and the electrical properties of epitaxial films with $x=0.16$ grown by metalorganic chemical vapor deposition (MOCVD) as well as the composition control method by MOCVD.

II. EXPERIMENTAL

xBiCoO$_3$–$(1-x)$BiFeO$_3$ solid-solution films were grown on (100)SrTiO$_3$ substrates at 500–700 °C by MOCVD using Bi[(CH$_3$)$_2$(2-(CH$_3$)$_2$NCH$_2$C$_6$H$_4$)] (Tosoh Corp.), Fe(C$_2$H$_5$C$_5$H$_4$)$_2$, Co(CH$_3$C$_5$H$_4$)$_2$, and oxygen gas as the source materials. A vertical type reactor maintained at a pressure of 530 Pa was used to prepare the films. The films were deposited using pulsed introduction of the mixture gases of Bi, Fe, and Co sources for 10 s at 5 s intervals (pulse-MOCVD). (100)SrTiO$_3$ substrates with an epitaxial SrRuO$_3$ layer for the bottom electrodes, $(100)_c$SrRuO$_3$‖(100)SrTiO$_3$, were also used to evaluate the electrical properties.[10]

Varying the input gas flow rate of each source gas adjusted the film composition via the following equation:

$$R\ (\text{source}) = \frac{P(T) \times l}{P_v}, \tag{1}$$

where R (source), $P(T)$, l, and P_v are the theoretical gas flow rate of the source gas, vapor pressure of the source at the fixed temperature (T), flow rate of the carrier gas, and the pressure of the source vessel, respectively.[11]

a)Electronic mail: funakubo@iem.titech.ac.jp.

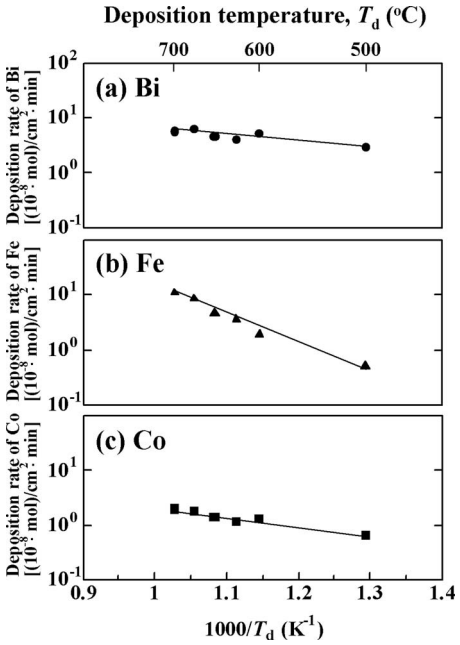

FIG. 1. Deposition rates of constituent metal elements: (a) Bi, (b) Fe, and (c) Co, as a function of the inverse of the deposition temperature under a fixed input gas flow rate of $R\{Bi[(CH_3)_2(2\text{-}(CH_3)_2NCH_2C_6H_4)]\}$ =20 cm^3/min, $R[Fe(C_2H_5C_5H_4)_2]$=60 cm^3/min, and $R[Co(CH_3C_5H_4)_2]$ =20 cm^3/min. Substrate: $SrTiO_3$.

Film compositions and the thickness were measured by x-ray fluorescence and scanning electron microscopy, respectively. The crystal structure of the deposited films was characterized by high-resolution x-ray diffraction (HRXRD) analysis using a four-axis diffractometer with Cu $K\alpha$ radiation. In addition, HRXRD-reciprocal space mapping (RSM) around $SrTiO_3$ 004 and 204 diffractions was employed for a detail analysis of the crystal structure.

The electrical properties, including the leakage current density-electric field (J-E) curves and the polarization-electric field (P-E) hysteresis loops, were measured at 80 K using a Pt/$[x BiCoO_3-(1-x)BiFeO_3]$/$SrRuO_3$ capacitor structure after depositing the platinum top electrodes with a 100 μm in diameter using an electric beam evaporation technique. The electrical properties were measured using a semiconductor parameter analyzer (HP4155B, Hewlett-Packard) and ferroelectric tester (FCE-1, Toyo Corporation).

III. RESULTS AND DISCUSSION

A. Composition control

In MOCVD, controlling the film composition is critical for constructing films with the desired x value in $xBiCoO_3-(1-x)BiFeO_3$, which consists of three metal elements. Figure 1 shows the deposition rate of each constituent element, Bi, Fe, and Co, prepared on a (100) $SrTiO_3$ substrate under a fixed input source gas concentration as functions of inverse deposition temperature from 500 to 700 °C. The deposition rate increased as the deposition temperature increased and nearly linear relationships with different slope were observed in Fig. 1, suggesting that the growth rate for each element has the same limitation step within this temperature range. Moreover, the different slopes in Fig. 1 suggest the film composition changes with deposition temperature.

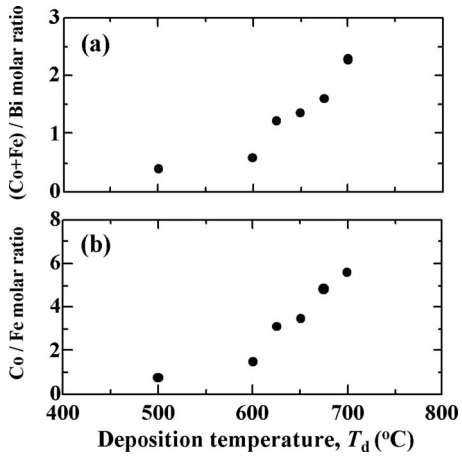

FIG. 2. (a) (Co+Fe)/Bi and (b) (Co/Fe) molar ratio as a function of deposition temperature replotted from the data shown in Fig. 1. Substrate is $SrTiO_3$

Figure 2 replots the data shown in Fig. 1 for the molar ratio of the [(Co+Fe)/Bi], which corresponds to the [(B-site)/(A-site)] ratio in a perovskite structure, ABO_3, and the molar ratio of (Co/Fe), which corresponds to the (Co/Fe) ratio in the B site as a function of deposition temperature. As shown in Fig. 2, both of [(Co+Fe)/Bi] ratio and (Co/Fe) ratio increased as the deposition temperature increased. These results indicate that the input gas flow rate of each source gas must be adjusted to realize films with the desired composition at a fixed deposition temperature.

Figure 3 shows the [(Fe+Co)/Bi] and [(Fe/Co) or (Co/Fe)] ratios as functions of theoretical input source gas flow rates of Fe and Co sources, $R[Fe(C_2H_5C_5H_4)_2]$ and $R[Co(CH_3C_5H_4)_2]$, for films prepared at 700 °C on (100)$SrTiO_3$ substrates. Both the [(Fe+Co)/Bi] and [(Fe/Co) or (Co/Fe)] ratios increased as the input gas flow rates of the Fe or Co sources increased, implying that controlling the composition of the input source gases can alter the film composition.

Figure 4 shows the deposition amount per unit area for the constituent elements of Bi, Fe, and Co as a function of deposition time for $0.16BiCoO_3-0.84BiFeO_3$ films grown at 700 °C on (100)$SrTiO_3$ and $(100)_cSrRuO_3\|(100)SrTiO_3$ substrates. Regardless of the type of substrate, a nearly linear relationship was observed between the deposition amount and deposition time, which demonstrates that film thickness can be controlled by adjusting the deposition time while maintaining the same film composition.

In the section below, the film thickness dependency of the crystal structure and the electrical properties were investigated for $0.16BiCoO_3-0.84BiFeO_3$ films deposited at 700 °C on (100)$SrTiO_3$ and $(100)_cSrRuO_3\|(100)SrTiO_3$ substrates.

B. Thickness dependence of crystal structure

Figure 5 shows HRXRD-RSMs around 004 and 204 for 55, 165, and 400 nm thick films grown on (100)$SrTiO_3$ sub-

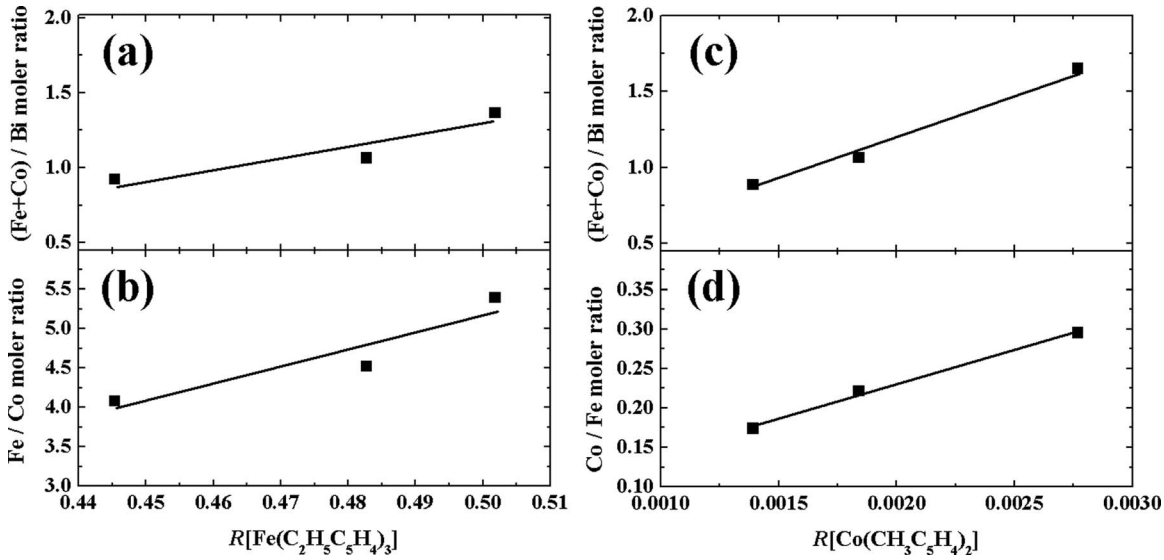

FIG. 3. [(a) and (c)] (Fe+Co)/Bi and [(b) and (d)] (Fe/Co) or (Co/Fe) molar ratio as a function of [(a) and (b)] $R[Fe(C_2H_5C_5H_4)_2]$ and [(c) and (d)] $R[Co(CH_3C_5H_4)_2]$ for films deposited at 700 °C. Substrate: $SrTiO_3$

strates. In the 55 nm thick film case, the 004 and 204 spots were each a single spot shown in Figs. 5(a) and 5(b). These spots were located at the same value along the surface normal direction, suggesting a 90° internal angle. Because the 004 spot was located only along the surface normal direction, this film has a tetragonal symmetry with an elongated axis along the surface normal direction because the inverse of the lattice spacing along the surface normal is longer than that along in-plane direction. In contrast, for the 400 nm thick film, both the 004 and 204 spots consisted of two spots shown in Figs. 5(e) and 5(f), which were located at the same value along surface normal direction. Based on the fact that the 004 spots were located off center from the surface normal direction with same tilting angle, this film has a rhombohedral symmetry because the internal angle is not 90° but the lattice spacings are basically the same. Details of the determination methods for rhombohedral and tetragonal symmetries are described in Refs. 5, 6, and 12. As shown in Figs. 5(c) and 5(d), the HRXRD-RSMs of the 165 nm thick films were a mixture of those for the 55 and 400 nm films, suggesting that these films consist of a mixture of the tetragonal and rhombohedral phases.

Figure 6 shows the HRXRD-RSMs around 004 and 204 diffractions for films with same thickness shown in Fig. 5 grown on $(100)_c SrRuO_3 \| SrTiO_3$ substrates. The open circles indicate spots from $SrRuO_3$ peaks. The thickness dependency of these films grown on $(100)_c SrRuO_3 \| SrTiO_3$ sub-

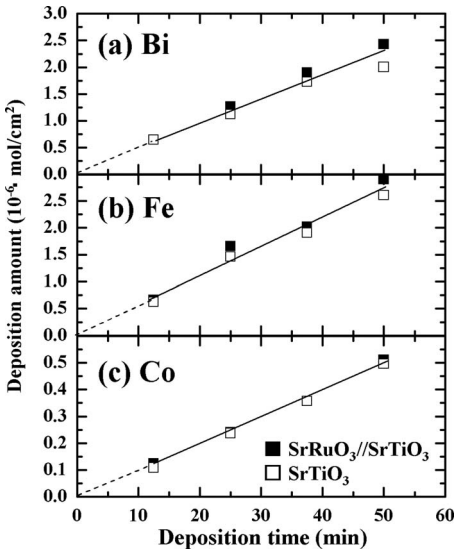

FIG. 4. Deposition amount of constituent metal elements as a function of deposition time. (a) Bi, (b) Fe, and (c) Co. Substrate: (□) for $SrTiO_3$ and (■) for $(100)_c SrRuO_3 \| (100)SrTiO_3$

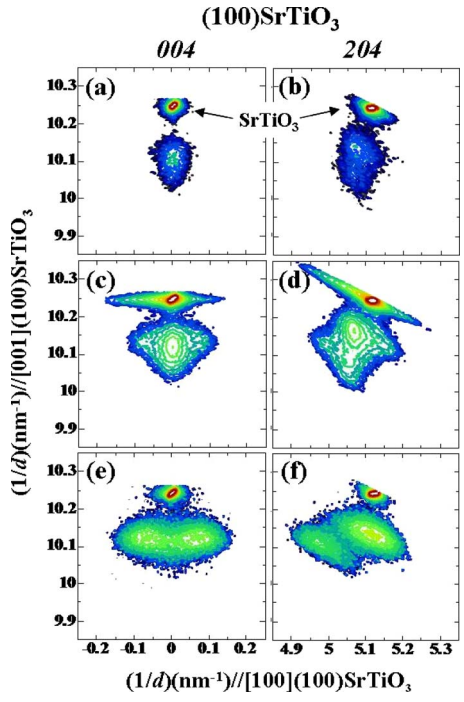

FIG. 5. (Color online) HRXRD-RSMs around [(a), (c), and (e)] $SrTiO_3$ 004 and [(b), (d), and (f)] $SrTiO_3$ 204 for $0.16BiCoO_3-0.84BiFeO_3$ films grown on $(100)SrTiO_3$ substrates. Film thickness: [(a) and (b)] 55 nm, [(c) and (d)] 165 nm, and [(e) and (f)] 400 nm.

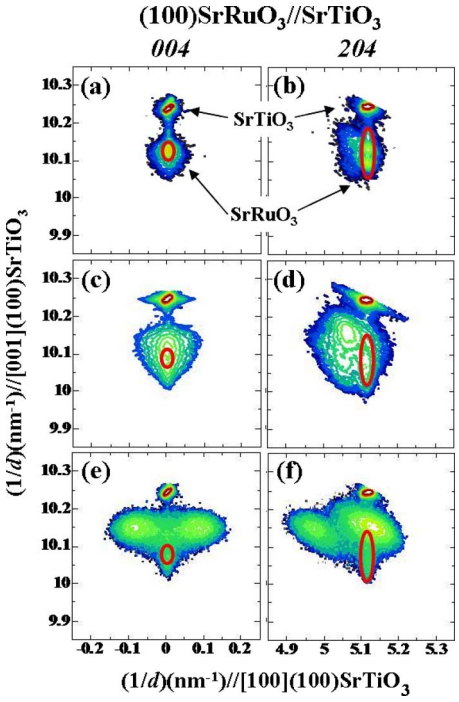

FIG. 6. (Color online) HRXRD-RSMs around [(a), (c), and (e)] $SrTiO_3$ 004 and [(b), (d), and (f)] $SrTiO_3$ 204 for $0.16BiCoO_3-0.84BiFeO_3$ films grown on $(100)_c SrRuO_3 \| (100)SrTiO_3$ substrates. Film thickness: [(a) and (b)] 55 nm, [(c) and (d)] 165 nm, and [(e) and (f)] 400 nm

strates was very similar to those on $(100)SrTiO_3$ substrates, which are shown in Fig. 5. The present data shown in Figs. 5 and 6 clearly indicate a crystal symmetry change with film thickness, regardless the type of the substrate, and suggest that change in the x values for the crystal symmetry boundaries between the tetragonal and rhombohedral symmetries is the same as that reported for $BiFeO_3$ and the $Pb(Zr,Ti)O_3$ films.[13,14]

Based on the phase diagram for the $BiCoO_3-BiFeO_3$ solid-solution system reported by Azuma *et al.*,[15] a film with a cubic symmetry was deposited at 700 °C for a $0.16BiCoO_3-0.84BiFeO_3$ film because the Curie temperature (T_c) is below 700 °C and likely transforms to the tetragonal one at T_c during the cooling process after deposition. In addition, this transformation was accompanied by an additional phase transition from tetragonal to rhombohedral symmetry prior to reaching room temperature. When the film was thicker than 400 nm, the crystal symmetry basically followed this phase diagram and had a rhombohedral symmetry at room temperature. However, the symmetry changed to tetragonal, even at room temperature, when the film became thin as shown in Figs. 5 and 6. Similar to the report for $BiFeO_3$ films, this change is most likely due to the increase in the clamping effect from the substrate as the film thickness decreases.[13]

C. Electrical properties

Figure 7 shows the leakage current density-electric field (J-E) curves measured at 80 K for the same films shown in Fig. 6. As the film thickness increased, the leakage current density decreased. Figure 8 shows the polarization-electric

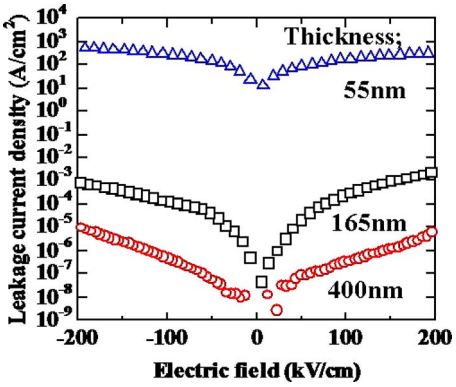

FIG. 7. (Color online) J-E curves of $0.16BiCoO_3-0.84BiFeO_3$ films with various thicknesses measured at 80 K. Substrate: $(100)_c SrRuO_3 \| (100)SrTiO_3$

field (P-E) hysteresis loops measured at 80 K under a 1 kHz frequency for a 400 nm thick film. Well saturated hysteresis loops were observed with remanent polarization (P_r) and a coercive field (E_c) of 62 $\mu C/cm^2$ and 180 kV/cm, respectively, at a maximum electric field of approximately 650 kV/cm. These values are smaller than that of $BiFeO_3$ films with the same film thickness due to the decreased crystal asymmetry as the x value increases.[6]

IV. CONCLUSION

Although the composition of $xBiCoO_3-(1-x)BiFeO_3$ films prepared by MOCVD changes with the deposition temperature, the composition can be controlled by adjusting the input source gas composition at 700 °C. $0.16BiCoO_3-0.84BiFeO_3$ films with various film thicknesses can be grown by altering the deposition time. In addition, for films grown on both $(100)SrTiO_3$ and $(100)_c SrRuO_3 \| (100)SrTiO_3$ substrates, the crystal symmetry changes from rhombohedral to the tetragonal symmetry as the film thickness decreases, implying that the x value where crystal symmetry changes from tetragonal to rhombohedral the x value shifts with film thickness. Well saturated hysteresis loops with $P_r=62$ $\mu C/cm^2$ and $E_c=180$ kV/cm are observed for 400 nm thick $0.16BiCoO_3-0.84BiFeO_3$ films.

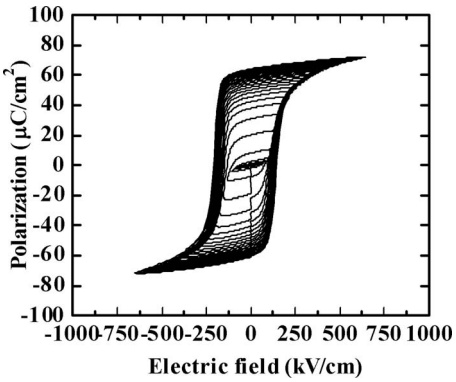

FIG. 8. P-E hysteresis loops of 400 nm thick $0.16BiCoO_3-0.84BiFeO_3$ films measured at 80 K at a 1 kHz frequency. Substrate: $(100)_c SrRuO_3 \| (100)SrTiO_3$.

ACKNOWLEDGMENTS

This work is supported by Grants-in-Aid from MEXT of Japan for Scientific Research (No. 07117022) and the Elements Science and Technology Project and Education and Research Center for Material Innovation in the Tokyo Institute of Technology Global COE Program.

[1]G. H. Haertling, J. Am. Ceram. Soc. **50**, 329 (1967).
[2]T. Takenaka and H. Nagata, Key Eng. Mater. **157**, 57 (1999).
[3]J. Wang, J. B. Neaton, H. Zheng, V. Nagarajan, S. B. Ogale, B. Liu, D. Viehland, V. Vaithyanathan, D. G. Schlom, U. V. Waghmare, N. A. Spaldin, K. M. Rabe, M. Wuttig, and R. Ramesh, Science **299**, 1719 (2003).
[4]Y. Saito, H. Takao, T. Tani, T. Nonoyama, K. Takatori, T. Homma, T. Nagaya, and M. Nakamura, Nature (London) **432**, 84 (2004).
[5]S. Yasui, K. Nishida, H. Naganuma, S. Okamura, T. Iijima, and H. Funakubo, Jpn. J. Appl. Phys., Part 1 **46**, 6948 (2007).
[6]S. Yasui, H. Naganuma, S. Okamura, K. Nishida, T. Yamamoto, T. Iijima, M. Azuma, H. Morioka, K. Saito, M. Ishikawa, T. Yamada, and H. Funakubo, Jpn. J. Appl. Phys. **47**, 7582 (2008).
[7]H. Naganuma, N. Shimura, J. Miura, H. Shima, S. Yasui, K. Nishida, T. Katoda, T. Iijima, H. Funakubo and S. Okamura, J. Appl. Phys. **103**, 07E314 (2008).
[8]B. Noheda, D. E. Cox, G. Shirane, J. A. Gonzalo, L. E. Cross, and S.-E. Park, Appl. Phys. Lett. **74**, 2059 (1999).
[9]B. Noheda, D. E. Cox, G. Shirane, S.-E. Park, L. E. Cross, and Z. Zhong, Phys. Rev. Lett. **86**, 3891 (2001).
[10]T. Kamo, K. Nishida, K. Akiyama, J. Sakai, T. Katoda, and H. Funakubo, Jpn. J. Appl. Phys., Part 1 **46**, 6987 (2007).
[11]T. Matsuzaki, N. Okuda, K. Shinozaki, N. Mizutani, and H. Funakubo, Jpn. J. Appl. Phys., Part 1 **37**, 6229 (1998).
[12]K. Saito, T. Oikawa, I. Yamaji, T. Akai, and H. Funakubo, J. Cryst. Growth **237–239**, 464 (2002).
[13]K. Saito, A. Ulyanenkov, V. Grossmann, H. Ressi, L. Bruegemann, H. Ohta, T. Kurosawa, S. Ueki, and H. Funakubo, Jpn. J. Appl. Phys., Part 1 **45**, 7311 (2006).
[14]S. Yokoyama, H. Morioka, Y. K. Kim, H. Nakaki, and H. Funakubo, J. Mater. Res. **22**, 1551 (2007).
[15]M. Azuma, S. Niitaka, N. Hayashi, K. Oka, M. Takano, H. Funakubo, and Y. Shimakawa, Jpn. J. Appl. Phys. **47**, 7579 (2008).